Report of AOARD Program

CONTRACT NO: FA23861014160

Miniaturized X-ray Generation by Pyroelectric Effect using Short Pulse Laser

Dr. Kenji Kitamura (PI)
Fellow
National Institute for Materials Science
1-1 Namiki, Tsukuba, 3050044 Japan

November 10th 2011

Contents

Report Documentation Page

Form Approved
OMB No. 0704-0188

1. REPORT DATE	2. REPORT TYPE	3. DATES COVERED
30 NOV 2011	**Final**	**02-09-2010 to 01-10-2011**

4. TITLE AND SUBTITLE
Enhancement of pyroelectric effect using short pulse laser aiming at miniaturized X-ray generator

5a. CONTRACT NUMBER
FA23861014160

5b. GRANT NUMBER

5c. PROGRAM ELEMENT NUMBER

6. AUTHOR(S)
Kenji Kitamura

5d. PROJECT NUMBER

5e. TASK NUMBER

5f. WORK UNIT NUMBER

7. PERFORMING ORGANIZATION NAME(S) AND ADDRESS(ES)
National Institute of Materials Science,Tsukuba,Ibaraki 305-0044,Japan,JP,305-0044

8. PERFORMING ORGANIZATION REPORT NUMBER
N/A

9. SPONSORING/MONITORING AGENCY NAME(S) AND ADDRESS(ES)
AOARD, UNIT 45002, APO, AP, 96338-5002

10. SPONSOR/MONITOR'S ACRONYM(S)
AOARD

11. SPONSOR/MONITOR'S REPORT NUMBER(S)
AOARD-104160

12. DISTRIBUTION/AVAILABILITY STATEMENT
Approved for public release; distribution unlimited

13. SUPPLEMENTARY NOTES

14. ABSTRACT
Ferroelectric crystals such as LiNbO3 (LN) and LiTaO3 (LT) are currently used as infrared sensors, electro-optical devices, nonlinear optical devices, X-ray generators, neutron generators, and tabletop nuclear fusion systems. We demonstrated fundamental measurements of pyroelectric current and surface charges accumulated by temperature change using ordinary heater, Pertier device and CO2 gas laser. Based on results, we shifted our target to surface potential caused by photogalvanic effect. We demonstrated photo-induced currents under a visible wavelength laser. The photogalvanic current was superior to the pyroelectric one under such conditions.

15. SUBJECT TERMS
Energy Conversion

16. SECURITY CLASSIFICATION OF:			17. LIMITATION OF ABSTRACT	18. NUMBER OF PAGES	19a. NAME OF RESPONSIBLE PERSON
a. REPORT	b. ABSTRACT	c. THIS PAGE			
unclassified	**unclassified**	**unclassified**	**Same as Report (SAR)**	**11**	

Introduction

Ferroelectric crystals such as $LiNbO_3$ (LN) and $LiTaO_3$ (LT) are currently used as infrared sensors, electro-optical devices, nonlinear optical devices, X-ray generators, neutron generators, and tabletop nuclear fusion systems.[1,2] On the surfaces perpendicular to the direction of ferroelectric spontaneous polarization, the **polarization charges** are exposed on the surface of crystal. In the air, however, these charges are almost compensated or neutralized by charges of ionized particles absorbed from the environment. They are called "**screening charges"**. With a temperature change, the spontaneous polarization is varied as a nature of pyroelectric material. The generation of electrons on the surface is explained qualitatively by the appearance of the uncompensated charges on the polar faces of the crystal during the thermal cycles to which the crystal is subjected.

However, the electric current caused by pyroelectric effect is proportional to the speed of temperature change. The current can be measured only while the crystal temperature is changing. When the crystal temperate is stable at any temperature, pyroelectric effect doesn't take place. It, therefore, is a key factor how fast the crystal temperature is changed to enhance the pyroelectric current and the charge accumulation on the surfaces of crystal.

In the conventional method, a thermal heater has been used. This method can heat the crystal up to a high temperature such as 400 ℃. However, the speed of heating is considerably slow. Moreover, rapid heating and cooling of such large temperature change causes a thermal shock and cracking of the crystal.

In this program, we proposed utilization of short pulse laser to heat the crystal. It can make only a small temperature change, but the temperature change is tremendously large comparing with that induced by an ordinary heater. We obtained some fundamental results on pyroelectric current induced by a short pulse (10 ns) green laser. It turned out that only 0.2 ℃ temperature change during 10 ns caused a giant current such as 20 mA. This value was $10^4 \sim 10^5$ times larger than the current usually obtained by using an ordinary heater. This fact looked promising the application of heating by laser for generating X-ray. From this background, we used CO_2 gas laser to heat LN. Through the experiments, we found a serious limit in heating the crystal by CO_2 gas laser.

We should note here that there are two photo-induced currents when ferroelectric crystal such as LN is irradiated. One is pyroelectric current which is generated during the temperature raising by laser irradiation and cooling after switching off the laser. The other is photogalvanic (= photovoltaic) current. Under laser irradiation, the excited electrons transfer one-directionally and continuously from –c to +c along the crystallographic c axis in LN. We re-calculated theoretically which current was dominant in our previous experiment using a short pulse (10 ns) green laser. We concluded that even under such a short pulse laser irradiation, photogalvanic current exceeded pyroelectric current. From this result, we shifted our target to surface potential caused by photogalvanic effect.

In this report, the contents were divided into two parts as:

Part I: Fundamental measurements of pyroelectric effects

Part II: Photo-induced currents by short-pulse high-power laser irradiation

References of Introduction

[1] Jamies D. Brownridge, "Pyroelectric X-raqy Generator" Nature, 358 (1992) 287

[2] J. D. Brownridge and S.M.Shafroth, "Self-focused electron beams produced by pyroelectric crystals on heating or cooling in dilute gases", Appl. Phys. Lett. 79 (2001) 3364

Part I: Fundamental measurement of ferroelectric effects

I-1: Pyroelectric current during temperature change using an ordinary heater

The polarization charges (= σ_{pl}) of ferroelectric crystal are exposed on the surfaces perpendicular to the direction of the spontaneous polarization. In air, however, these charges are almost compensated or neutralized by "screening charges (= σ_{sc})" which originate from ionized particles absorbed from the environment [1]. The spontaneous polarization (Ps) varies with temperature depending on the nature of the pyroelectric material, and the generation of electrons at the surface is explained qualitatively by the appearance of uncompensated charges on the polar faces of the crystal during thermal cycles.

When two opposing polar surfaces are electrically connected, a pyroelectric current can be measured with an ammeter during a temperature change. The pyroelectric current density J_{pyro} can be simply expressed as

$$J_{pyro} = -\delta Ps/\delta t = -(\delta Ps/\delta T)(\delta T/\delta t) = p(\delta T/\delta t) \qquad (1)$$

where t and T are time and temperature, respectively, and $p = \delta Ps/\delta T$ is the pyroelectric coefficient. Equation (1) suggests that J_{pyro} is proportional to the rate of temperature change. The current is thus present only when the crystal temperature is changing, so the rate of temperature change becomes a key factor in determining the enhancement of the pyroelectric current.

In the conventional method, a thermal heater is used to heat the crystal (e.g., Ref. [2]). The heater or heat-gun method can heat the crystal to temperatures as high as 400 °C [3], but the rate of heating is rather slow. Figure I-1a shows a set-up for measuring pyroelectric current using LN plate perpendicular to the Ps direction. The LN plate was Cu-coated on the both +c and –c surfaces. Figure I-1b shows the result of measurement. Although the LN plate was heated up to 500 ℃, only 200 nA current was observed as a maximum during the heating[3]. The maximum temperature change was around 20 ~ 30 °C/sec. After turning off the heat-gun, the crystal was cooled faster and smoothly than heating. Even though only 300 nA current was observed as a maximum during the cooling.

In the conventional heating method, there is a limit of temperature changing rate. Too rapid heating and cooling over such large variations in temperature can result in thermal shock and cracking of the crystal.

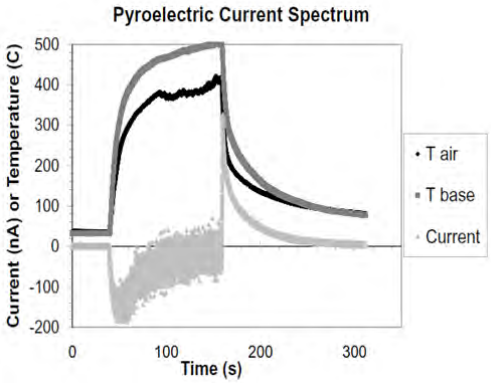

Fig. I-1a (left):Set-up for pyroelectric current measurement using LN crystal plate heated by a heat-gun. The crystal faces are perpendicular to the c polarization direction and coated by Cu [3].

Fig. I-1b (right): Pyroelectric current observed using a heat-gun heater. Grey line shows the temperature of air on the surface blowed on by the heat-gun and black line shows one at the opposite bottom surface [3].

I-2:Pyroelectric current using CO_2 gas laser as heater

$LiNbO_3$ crystal (LN) exhibits a huge absorption coefficient for IR light with a wavelength over 6 μm. We used a CO2 gas laser (wave length:10.6 μm, Max. CW power: 5W, Model Lasy-5P Access Laser) as a heater. Figure I-2 shows the set-up of LN crystal (10 mm x 10 mm x 0.5 mm thickness) whose +c and –C surfaces are coated by ITO of 100 nm thickness. The crystal is cramped by Cu blocks as electrode. The incident face is directly grounded, and the opposite face is grounded through an ammeter.

The crystal was heated by the laser for 40 second and cooled in air. Figure I-3 shows the pyroelectric current measured by the CO_2 gas laser irradiation. A and B indicate the currents when the laser incident face was grounded as shown in Figure I-2. C shows the current when the incident face was not grounded. It is noteworthy that the current of C is about a half of A and B.

In any case, the currents during heating and cooling are symmetric along the opposite directions to each other. The cooling rate is dominated by a heat escape from the surfaces and the thermal conduction of crystal. Because the currents during heating and cooling are the same (along the opposite directions), $\delta T/\delta t$ during heating is almost equal with $-\delta T/\delta t$ during cooling.

The peaks of A and B were ~40 nA. They were at the same level with the current value measured by the heat-gun method.

By the CO_2 gas laser irradiation with a long wavelength of 10.6 μm, only the surface is heated since the light cannot penetrate deeply into the crystal. The heat transfer mechanism by the CO_2 gas laser irradiation is almost the same with that by heating using a heat gun.

A serious problem of the CO_2 gas laser heating was it caused too large thermal gradient in the crystal. As a result, LN samples were cracked by the irradiation with a larger intensity than 1W.

As a result, we concluded that heating by CO_2 gas laser is not available to generate pyroelectric current or to accumulate surface charges although the laser light can be delivered by using optical fibers flexibly. The absorption coefficient of LN for CO_2 gas laser wavelength is extremely too large.

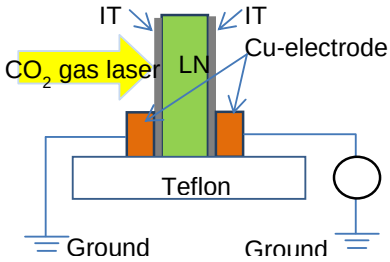

Fig. I-2: Setup of sample mounting for CO_2 gas laser irradiation.

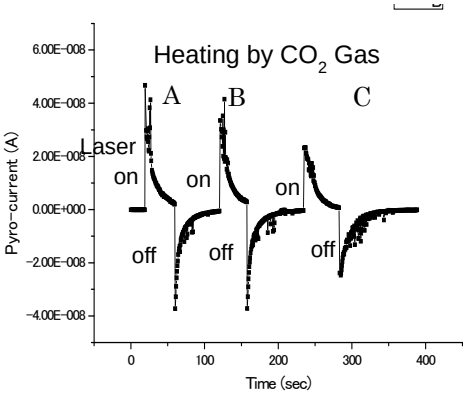

Fig. I-3: Pyroelectric currents heated by CO_2 gas laser. They exhibit a pair of currents during heating and cooling. C indicates that even when the incident face is not grounded, a half of current (grounded, A and B) can be measured

I-3: Surface potential accumulated by pyroelectric effect on polar surface

We measured the voltage on LN polar surfaces (+c and –c faces) to characterize quantitatively the surface potential using surface voltage sensor. LN samples were prepared as to be a disc of 8 mm diameter and 0.5 mm thickness. On the one face, Cr was coated in a diameter around 5 mm. As shown in Figure I-4, the periphery of the disc was covered by manicure paste to avoid discharge of accumulated charges from one face to the other.

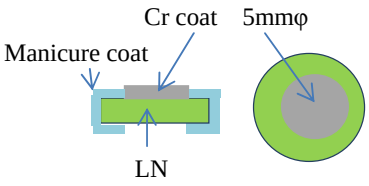

Fig. I-4: Sample preparation of LN disc.

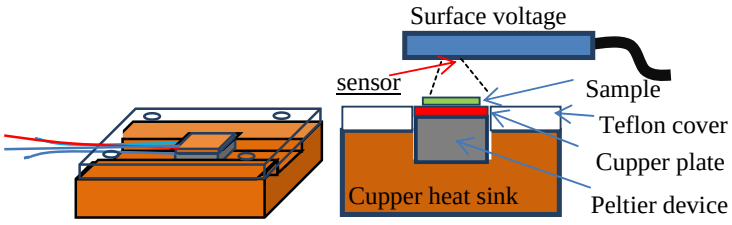

Fig. I-5: Pertier device for sample heating and cooling.

The disc sample was put on a Pertier device as shown by Figure I-5. By a program controller, the Pertier device can heat and cool the sample rather quickly, for example, 1 /sec. Figure I-5 also shows the set-up of a surface voltage sensor above the sample.

Figure I-6 shows the surface voltages measured when the sample was heated. It suggests that even 10 ℃ rise of temperature from 25 ℃ generate around 400 V.

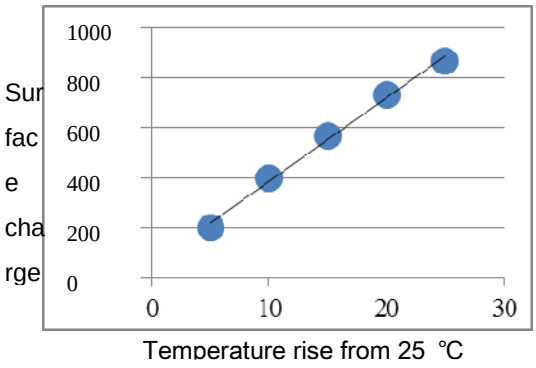

Fig. I-6: Surface voltage and temperature rise from 25 ℃.

Figure I-7 shows the potential change on +c LN surface according to the temperature change programed. When the temperature raised from 25 ℃ to 30 ℃, the negative potential increased up to ~ - 200V. While the temperature is held during 60 seconds, the potential didn't obviously change. When the temperature was lowered to 25 ℃, the potential returned to the initial level. Next, when the temperature was lowered to 20℃ after holding 60 seconds, the potential increased positively around 200V. While the temperature was kept at 20℃ for 90 seconds, the potential was slightly decreasing. When the temperature was raised to the initial room temperature, the potential returned to the initial level.

This result suggests that the potential changes rather quickly following the temperature change. And when the temperature is held at a certain temperature with some potential, the potential (excess screening charge) is not neutralized, that is, the neutralization needs rather long time.

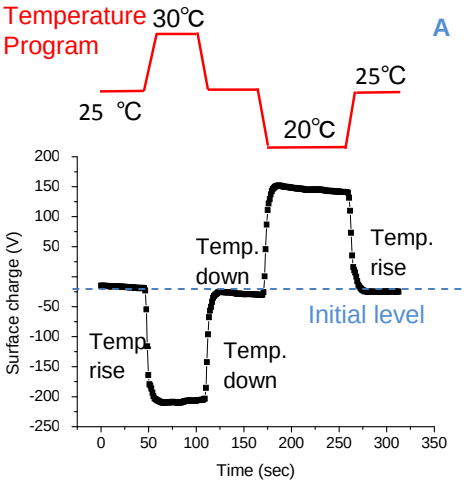

Fig. I-7: Remaining surface charges. By controlling discharges, the surface charges remain for a long period.

References of Part I

[1] X. Liu, K. Kitamura and K. Terabe, Appl. Phys. Lett. **89**, 132905 (2006).

[2] J. D. Brownridge, S. Raboy, J. Appl. Phys. **86**, 640 (1999).

[3] P. R.Wali, K. O'Doherty and J. K. Gimzewski, unpublished

Part II: Photo-induced currents by short-pulse high-power laser irradiation

II-1: Experiments and results

An Fe-doped $LiNbO_3$ crystal (about 600 ppm Fe) was cut and polished to form a plate with polar faces perpendicular to the Z axis and with dimensions of 10 × 10 × 0.5 mm^3. Both $+Z$ and $-Z$ faces were coated by 10-nm-thick indium-tin-oxide (ITO) films with no antireflection coating. The sample was clamped vertically on a Teflon plate with two small brass blocks that also served as electrodes (Figure II-1). One electrode was connected to an oscilloscope and the other was grounded. A high-power green (wavelength 532 nm) pulsed laser, with a pulse width and repetition rate of 10 ns and 10 Hz, respectively, was used to irradiate the sample (Figure II-2). The profile of the photo-induced current, J , was measured with sub-nanosecond time resolution using an oscilloscope.

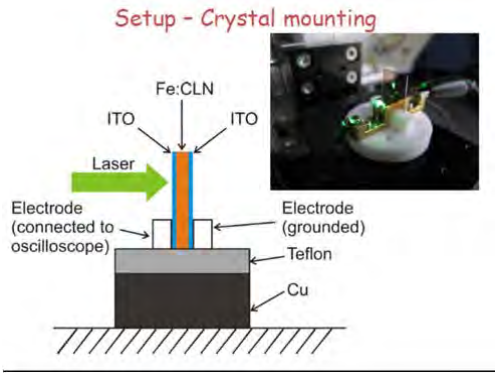

Fig. II-1: Sample mounting for photo-induced current measurement by laser irradiation

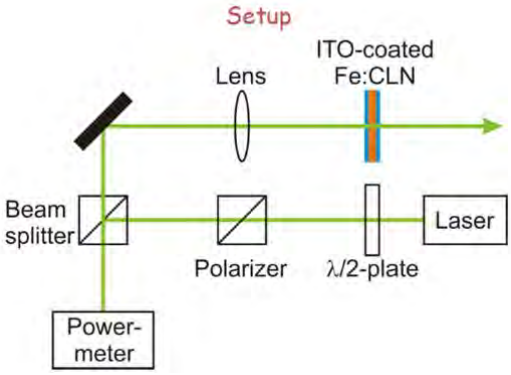

Fig. II-2: Optical set-up for photo-induced current using a high-power pulse laser

Figure II-3 shows that the peak photo-induced current was linearly related to the light power incident on the crystal, which we defined as the peak laser intensity multiplied by the irradiated area The beam diameter (at $1/e^2$ of the peak power) was 4.25 mm, and the peak power was varied from 0.5 to 8 × 10^5 W. At the highest power, we observed a peak current of 25 mA, which was huge compared to the hundreds of nanoamperes or several microamperes that were observed when heating with a heat gun.

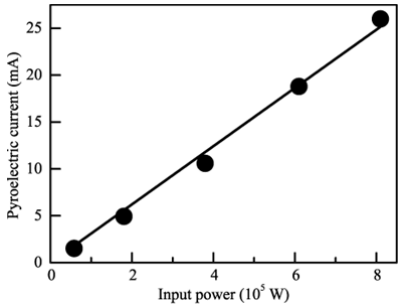

Fig.II-3: Photo-induced current as a function of laser irradiation power.

Figure II-4 shows the relationship between the photo- induced current and the irradiated area for constant power densities of 4 and 2 × 10^6 W/cm^2. The beam waist was varied from 0.7 to 1.8 mm, which translates into a variation in irradiated area on the crystal surface from 0.4 to 2.5 mm^2. These data are demonstrating that for a constant power density, the photo-induced current is proportional to the irradiated area. The sample size does not influence the photo-induced current in this method, which means that the photo-induced current is generated only in the irradiated area by the laser beam.

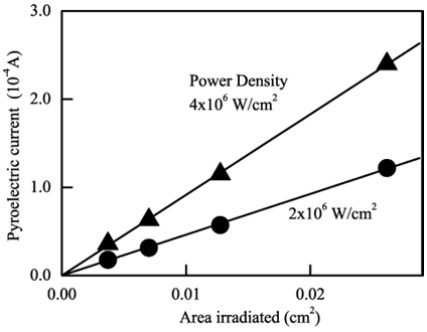

Fig.II-4: Dependence of photo-induced current on beam area for two different power densities.

Figure II-5 shows the time-dependent the photo-induced current when irradiated by a pulse with intensity 6 × 10^6 W/cm^2. During the 10-ns irradiation period, the crystal was heated. The data show that even after the 10-ns irradiation, the current decreased but existed, which indicates that the crystal temperature was still increasing some 30 ns after the laser irradiation.

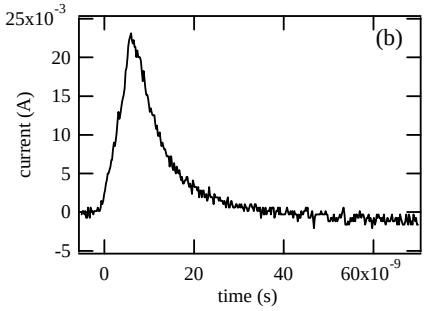

In addition, we found that the current in the opposite direction, which is usually observed in a pyro-electric current measurement while the crystal cools, was very small. We detected this small, oppositely directed current from about 30 ns after irradiation, and it

Fig.II-5 (right) : Time dependence of photo-induced current

lasts until approximately 300 ns before dropping below the noise level. In other words, upon irradiation with a 10-ns laser pulse, the crystal cooling for LN takes approximately 300 ns.

II-2: Theoretical calculations ~Analysis of currents induced by laser irradiation~

Our experiments revealed that a 10 ns 532 nm laser pulse with I=6 MW/cm^2 produced the electric current achieving a maximum of ≈23 mA in Fe-doped crystal of the area A=0.56 cm^2 and thickness L=0.05 cm.

In accordance with the photorefractive theory[1,2], the total current through an irradiated specimen including (i) photogalvanic, (ii) pyroelectric and (iii) photoconductive (electron diffusion) mechanisms can be calculated as:

$$J = J_{PG} + J_{Pyr} + J_d . \quad (1)$$

For the above experimental geometry the related components are written as:

$$J_{PG} = As(N_d - N_d^+)GI, \quad (2) \qquad J_{PYR} = -Ap \times dT / dt \quad (3) \qquad J_D = -Aq_e \mu N_e E, \quad (4) \; Aq_e D \nabla N_e$$

where N_d is the donor density, N_d^+ is the ionized donor density, N_e is the electron density, s is the absorption cross-section, G is the Glass constant, I is the laser radiation intensity, $p=dP/dT$ is the pyroelectric constant, μ is the electron mobility, D is the electron diffusion coefficient, E is the local electric field, q_e is the electron charge and E is the electric field defined via the local charge density as , $\nabla (\kappa\varepsilon_0 E + P) = q_e \Sigma N$, where κ is the dielectric constant and P is the polarization.

In order to estimate the value of J one should take into account that under laser intensity I=6 MW/cm^2 the initial donor density, N_d, can be depleted by the photo-ionization, as shown by the most simplistic estimate, i.e. $\Delta N_d \approx \Delta N_e \approx \alpha I \tau_p / h\nu \approx 1.7 \times 10^{18}$ cm^{-3}, where $\alpha = sN_d \approx 12$ cm^{-1} is the linear absorption coefficient associated with donors, $N_d \approx 10^{17}$ cm^{-3} is the characteristic donor density, $h\nu = 3.73 \times 10^{-19}$ J ≈2.33 eV is the photon energy and τ_p=10 ns is pulse duration. A more detailed estimate can be made by assuming electric charge quasi-neutrality, $N_e \approx N_d$, $\gamma N_e N_d^+ \approx \gamma_R N_d^{+2}$ giving for the recombination rate of electrons and ionized donors under which their density is described by:

$$\frac{dN_d^+}{dt} \approx \frac{sI}{h\nu}\left(N_d - N_d^+\right) - \gamma_R N_d^{+2} \quad (5)$$

where γ_R is the recombination rate constant.

In treating Eq. (5) one finds that the crucial role for level and related currents (3) - (4) is played by the recombination constant γ_R. Ref. [1] gives for this parameter γ_R =2.5x10^{-7} cm^3/s whereas our analysis suggests a significantly lower value for the above experiment. In particular, the value of γ_R is defined via the product of the cross-section, σ, and the mean electron velocity,

$$\langle V_e \rangle = (3k_B T_e / m_e)^{1/2} \;:\; \gamma_R = \sigma \langle V_e \rangle . \quad (6)$$

We use a possible minimal value for σ ≈ 2x10^{-16} cm^2 corresponding to the typical atomic cross-section. One can argue this value assuming that the effective electron-ion collision area can be extended by the electric field via which the migrating electron can “feel” the presence of the photo-ionized atom. However, this field, $E_l \approx q_e / 4\pi\kappa\varepsilon_0 r^2$, decays very sharply with increase in r towards the value comparable to that existing inside LN crystal, $E_p \approx P_s / \kappa\varepsilon \approx 10^7$ V/cm, estimated via the related spontaneous polarization P_s = 62 μC/cm^2 and κ =29-84[3]. Moreover, the additional charge leads also to the local rearrangement of the neighboring lattice atoms which induces the electrostatic screening of the photo-ionized atom.

Now let us estimate the electron velocity. Immediately after ionization by the incident photon,, the electron has a kinetic energy $Fe^{2+} + h\nu + 2 \rightarrow Fe^{2+} + e$, the electron has a kinetic energy $\varepsilon_{e0} \approx h\nu - E_d \approx$ 0.3-0.8eV (see energy diagram Fig. 2) where $E_d \approx$1.5 - 2 eV is the energy gap of the donor Fe^{2+} below the conduction band [4] and, therefore, the initial velocity $\langle V_e \rangle \approx$ (0.3-0.5)x10^8 cm/s could give for $\gamma_R \approx$ (0.36÷0.6)x10^{-8} cm^3/s and for the

minimal recombination time 1.7÷2.8 ns (when cm^{-3}). However, prior to the recombination the electron can travel over the distance of 0.05 cm experiencing $\approx 10^6$ interactions with the crystal lattice atoms and, therefore, (i) getting the energy from the laser irradiation and also (ii) dissipating it to the crystal lattice.

The change of electron energy with time due to the laser irradiation can be evaluated as:[20]

$$\frac{d\varepsilon_e}{dt} \approx 2\varepsilon_{osc}\frac{\omega^2\nu_{e-ph}}{\omega^2+\nu_{e-ph}^2} \approx 2\varepsilon_{osc}\nu_{e-ph} \approx \quad 7.2\text{x}10^5 \text{ eV/s}, \quad (7)$$

where $\varepsilon_{osc} = q_e E_l^{\,2}/(m_e\omega^2)$ is the electron quiver energy, $E_I \approx 19\sqrt{I} = 4.65\text{x}\,10^4$ V/cm is the electric field of laser radiation for $I = 6\text{x}10^6$ W/cm^2, m_e is the mass of electron, $\omega = 3.54\text{x}10^{15}$ rad/s and $\nu_{e\text{-}ph} \approx 5\text{x}10^{12}$ Hz is the characteristic electron-phonon collision frequency.

Using Eq. (7) one finds that the related energy increase, $\Delta\varepsilon_e \approx 2\varepsilon_{osc}\nu_{e\text{-}ph}\tau_P \approx 7.2\text{x}10^{-3}$ eV, is negligibly small. In contrast with this small effect, the initial electron energy can be effectively dissipated to the crystal lattice as defined by:

$$d\varepsilon_e/dt = -(\varepsilon_e - \varepsilon_l)/\tau^* \approx -\varepsilon_{e0}/\tau^* \approx -(1.5\div 4)\,\text{x}10^{12}\text{ eV/s}, \quad (8)$$

where ε_l is the crystal lattice energy, $\tau^* = \nu_{e\text{-}ph}^{-1} \approx 2\text{x}10^{-13}$ s is the characteristic relaxation time.

Eq. (8), i.e. , $\varepsilon_e(t) \approx \varepsilon_l + (\varepsilon_{e0} - \varepsilon_l)\exp(-t/\tau^*)$, suggests that the initial electron energy is dissipated to the lattice within the period $\delta t \approx 1$ ps after ionization. Therefore, $T_e \approx T_t \approx 300$ K and $\langle V_e\rangle \approx 1.2\text{x}10^7$ cm/s, which together with $\sigma \approx 2\text{x}10^{-16}$ cm^2 finally gives:

$$\gamma_R = \sigma\langle V_e\rangle \approx 2.4\text{x}10^{-9}\,\text{cm}^3/\text{s}.$$

The related recombination time can attain the value of $\tau_R \approx (\gamma_R N_d^{+})^{-1} \approx 4$ ns and the recombination can have an effect for ns laser pulses. Assuming I to be constant over the pulse duration the integration of Eq. (5) gives:

$$N_e(t) = N_d^+(t) = -\frac{aI}{2} + \left(bI + \frac{(aI)^2}{4}\right)^{1/2} \times \frac{ce^{2[bI+(aI)^2/4]^{1/2}\gamma t} - 1}{ce^{2[bI+(aI)^2/4]^{1/2}\gamma t} + 1} \quad (9)$$

where $a = \alpha/h\nu\gamma_R(N_d - N_a)$, $b = \alpha/h\nu\gamma_R$ and $c = \dfrac{\left(bI+(aI)^2/4\right)^{1/2} + aI/2}{\left(bI+(aI)^2/4\right)^{1/2} - aI/2}$

Using $\gamma_R \approx 2.4\text{x}10^{-9}$ cm^3/s we obtain that at middle of the laser pulse, t=0.5τp=5 ns, the ionized donors density reaches the steady-state level value:

$$N_d^+ \approx (bI + (\alpha I/2)^2)^{1/2} - \alpha I/2 \approx 0.9\text{x}10^{17}\,\text{cm}^{-3},$$

and for the photo-galvanic current we obtain the following value:

$$As\,(Nd - N_d^+)GI \approx 16\text{ mA},$$

where $G \approx 4\text{x}10^{-9}$ cm/V [3,4].

Now let us estimate the temperature change of the crystal over the laser pulse duration. For a crystal with the thickness L=0.05 cm temperature equalization by heat conductance (k=0.046 W/cm K) across L will continue 0.15 s and, therefore, for 10 ns pulse duration the effect of is negligibly small. Taking into account the change of the absorption over the pulse duration

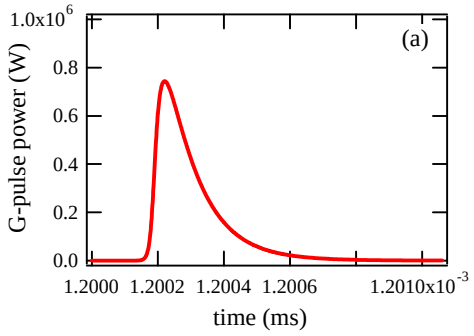

Fig.II-6: Pulse power of Q-switch YAG laser, the profile of power is well consistent with the time dependent profile of photo-induce current (Fig. II-5)

the temperature change is given by: $dT / dt \approx s(N_d - N_d^+)I/\rho c$ (10)
where c=650 J/kg K and ρ=4600 kg/m^3.

Thus, for $N_d^+ \approx 0.9\text{x}10^{17}$ cm^{-3} we find $dT / dt \approx 2.4\text{x}10^6$ K/s at the front of the crystal. In estimating I at the rear side of the crystal we have to take into account the absorption factor $\approx \exp[-s(N_d - N_d^+)L] \approx 0.94$ giving for $dT / dt \approx 2.3\text{x}10^6$ K/s and, therefore, we have:

$$J_{PYR} = -Ap \times dT / dt \approx 11 \text{ mA},$$

where p=-83x10^{-10} C/cm^2 K.[5]

The final temperature increase in the crystal $\Delta T \approx \tau_p dT / dt \approx 0.024$ K leads to $\delta P_s \approx -2 \times 10^{-10}$ C/cm^2. Additionally, in Fig. 1 b the laser induced current is found to extend over ≈30 ns. This effect can be attributed to the long energy tail of the 1.064 μm Q-switched laser used for obtaining 532 nm radiation pulse from a second harmonic generation crystal. Typically such energy tails extend pulses to ≈ 3 mid-amplitude periods[6] agreeing well with the observed current duration $3t_p$=30 ns.

For Eq. (4) we have $N_e \approx N_d^+$ and $\nabla(\kappa\varepsilon_0 E + P) \approx 0$. In fact, the calculation of N_e should take into account the additional term of the linear recombination of electrons with the acceptors [1], i.e. $\gamma_R N_a N_e$, where $N_a \approx 0.1 N_d$ is the acceptor density. However, for the considered case this term can be neglected due to $\gamma_R N_a \approx 2.4\text{x}10^7 \text{s}^{-1} << sI/h\nu \approx 1.9\text{x}10^9$ s^{-1}. Therefore, the value ∇N_e of can be obtained via $N_e \approx N_d^+$ and the characteristic length scale, $l \approx 1/s(N_d - N_d^+)$, as:

$$\nabla N_e \approx -N_e / l \approx -s(N_d - N_d^+) N_e \approx -1.1\text{x}10^{17} \text{ cm}^{-4}. \quad (11)$$

Using $D = \mu k_B T/q_e$ and μ=0.8 cm^2/Vs we find for the electron diffusion current:

$$J_D = A\mu k_B T \nabla N_e \approx 0.2 \text{ mA}.$$

Neglecting this contribution we finally find for the total current:

$$J = J_{PG} + J_{PYR} + J_D \approx J_{PG} + J_{PYR} \approx \mathbf{16} + 11 \approx 27 \text{ mA},$$

which agrees well with the maximum experimental value $J \approx 23$ mA and is fully consistent with the conclusion of Ref. [1] that **even under pulsed laser heating the pyroelectric mechanism can be comparable with the photogalvanic mechanism.**

By repeating our calculations for γ_R=2.5x10^{-7}cm^3/s [1] we find: $N_d^+ \approx 2.48\text{x}10^{16}$cm^{-3} and $dT/dt \approx 1.15\text{x}10^7$ K/s leading to $J_{PG} \approx 77$ mA, $J_{PYR} \approx 54$ mA and the resulting total current $J_{PG} + J_{PYR} \approx 131$ mA which exceeds the experimental value by ≈ 6 times. In making these estimates for I , we have to take into account the radiation absorption factor $\exp[-s(N_d - N_d^+)L] \approx 0.64$ at the rear side of the crystal. The above values are obtained for α = 12 cm^{-1}, and $N_d \approx 10^{17}$ cm^{-3} corresponding to 1.2x10^{-16}cm^2. However, Refs.[3, 7] suggest that for Fe^{2+} the absorption cross-section can be of order $s = 10^{-17}$ cm^2. Using this value we find for $N_d = \alpha/s \approx 1.2\text{x}10^{18}$ cm^{-3}, and by repeating our calculations for γ_R=2.4x10^{-9} cm^3/s we find: $N_d^+ \approx 2.52\text{x}10^{17}$cm^{-3} and $dT/dt \approx 1.18$x107 K/s, $J_{PG} \approx 79$ mA, $J_{PYR} \approx 55$ mA and $J \approx J_{PG} + J_{PYR} \approx 134$ mA. For $N_d \approx 1.2\text{x}10^{18}$ cm^{-3} and γ_R=2.5x10^{-7} cm^3/s, the calculations give: $N_d^+ \approx (\alpha I/h\nu\gamma_R)^{1/2} \approx 2.75\text{x}10^{16}$cm^{-3}and $dT/dt \approx 1.32\text{x}10^7$ K/s leading to $\approx J_{PG} \approx 88$ mA, $J_{PYR} \approx 61$ mA and $J \approx J_{PG} + J_{PYR} \approx 149$ mA.

II-3: Electric field induced by laser

Finally, let us consider the effect of electric field induced by the laser induced current $J \approx 27$ mA. This field is estimated as $E^* = J/A\sigma_{com} \approx 5 \text{ x } 10^3$ V/cm through the related value of the electrical conductivity $\sigma_{com} \approx q_e^2 N_e \nu_{e\text{-}ph}/m_e\omega^2$ where $Ne \approx 0.9\text{x}10^{17}$ cm^{-3} and $\omega = 2\pi\nu \approx 3.54 \text{ x } 10^{15}$ rad/s. During the relaxation time $\tau^* = \nu_{e\text{-}ph}^{-1} \approx 2\text{x}10^{-13}$ s this field increases the electron velocity on $\delta V \approx q_e E^* \tau^* / m_e \approx 1.7 \text{ x } 10^6$ cm/s which does not lead to a significant change in J. The above estimates suggest that higher laser intensities and related electric fields $E^* \approx 10^5 - 10^6$ V/cm are able to increase the electron velocity and the recombination rate constant to the level of $\gamma_R \approx 10^{-8} \div 10^{-7}$ cm^3/s. However, additionally to this effect the electrons with $\langle V_e \rangle \geq 1.2 \text{ x } 10^8$ cm/s having $\varepsilon_e \geq E_g \approx 4$

eV are able to start the electron avalanche ionization changing also the main equations for electrons and ions generation rate.[8]

II-4: Conclusions from theoretical calculations

We observed experimentally the current in Fe-doped $LiNbO_3$ generated by 532 nm wavelength laser pulse. We can conclude that it is attributed to the coupled action of the photogalvanic and pyroelectric mechanisms. Under 10 ns pulsed laser irradiance of $6x10^6$ W/cm^2 the electron energy rapidly dissipates the lattice and electron temperature reduces to $T \approx 300$ K resulting in low recombination rate constant $\gamma_R \approx 2.4x10^{-9}$ cm^3 which leads to a good agreement of the theoretically found electric current , 27 mA, with that of the experiment.

The results and theoretical discussions have revealed some important instructions to explain the phenomena observed by our experiments and for future directions of R&D using photo-induced electric effects in/on ferroelectric crystals.

First, **we found the fact that even though we used very short pulse such as 10 ns of irradiation, the photogalvanic current component exceeded the pyroelectric one.** The pyroelectric current is transient during the temperature change. At a constant temperature, no pyroelectric current occurs. However, the photogalvanic current flows continuously while the light is irradiating the crystal as shown in Figure II-7. It means, the total photogalvanic current is much superior to the pyroelectric one under the irradiation by a laser with longer pulse duration or CW laser.

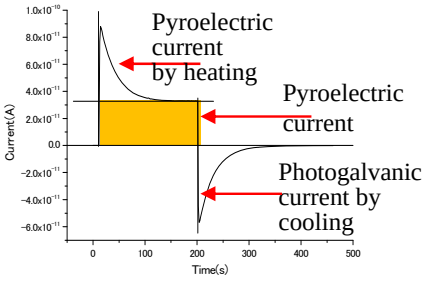

Fig. II-7: A typical time-dependent profile of photo-induced currents measured under the irradiation of CW green laser (500 mW) on Fe-doped LN.

We should note that there is more important difference between pyroelectric current and photogalvanic one. In case of pyroelectric effect, the current is a carrier transport of screening charges, i.e. charges of absorbents on the surface. There is no carrier transport through the crystal. Therefore, the pyroelectric current and charge accumulation on the surface strongly depend on the atmosphere. In contrast, the photogalvanic current is a flow of carriers excited by photons through the crystal. It doesn't depend on the atmosphere, even in air neither in vacuum. If the opposite surface is grounded (or connected with carrier source), photogalvanic current continues during the light irradiation. This fact suggests that the photogalvanic effect is very advantageous for charge accumulation on the polar surface for electron emission and other applications mentioned later.

References of Part II

[1] N. V. Kukhtarev, T.V. Kukhtareva, G. Stargell and J. C. Wang, J. Appl. Phys. 106, 014111 (2009).

[2]N. V. Kukhtarev, V. B. Markov, S. G. Odoulov, M. S. Soskin, and V. L. Vinetskii, Ferroelectrics 22, 949 (1979).

[3] T. Volk and M. Wöhlecke, *Lithium Niobate*, (Springer, Berlin Heidelberg 2010) and refs. therein

[4] H. Hatano, Y. Liu, and K. Kitamura, *in Photorefractive Materials and Their Applications II: Materials* , Eds: P. Gunter and J. P. Huignard, (Springer-Verlag, Berlin Heidelberg, 2007) p.127.

[5]Landort-Böernstein New Series III/29b, *Low Frequency Properties of Dielectric Crystals*, Ed. D. F. Nelson, (Springer-Verlag, Berlin Heidelberg 1993), p. 334.

[6]O. A. Louchev, Y. Urata, and S. Wada, *Optics Express* 15, 3940 (2007).

[7] S. A. Basun, D. R. Evans, T.J. Binning, S. Guha, J. O. Barnes, G. Cook, and R. S. Meltzer, J. Appl. Phys. 92, 7051 (2002).
[8] E. G. Gamaly, A. V. Rode, B. Luther-Davies, and V. T. Tikhonchuk, Physics of Plasmas 9, 949 (2002).

III. Summary and Acknowledgment

In Part I, we demonstrated fundamental measurements of pyroelectric current and surface charges accumulated by temperature change using ordinary heater, Pertier device and CO_2 gas laser. Because pyroelectric current depends on the temperature changing rate, large current cannot be expected by slow heating and slow cooling. We tried to heat LN crystal by using CO_2 gas laser. The absorption of LN at the wavelength of CO_2 gas laser, around 10 μm, is very large. We thought we could heat LN crystal so quickly. However, the absorption was too large and only the surface of sample was heated. It caused a big thermal gradient through the sample. It easily caused cracking of crystal under less than 1W intensity light.

By using Pertier device and surface voltage meter, we demonstrated how large surface potential could be accumulated on the crystal surfaces and how long such surface charges could remain on the surface without discharge. It turned out that the charged surface was not so quickly neutralized.

In Part II, we demonstrated photo-induced currents under a visible wavelength laser. We used a short pulse (10 ns) high power (~ $10^6 W/cm_2$) green laser. We measured a huge current such as 20 mA which was 5 orders of magnitude larger than the pyroelectric current obtained by heating using ordinary heaters.

We analyzed theoretically this huge photo-induced current. It turned out that the photogalvanic current was superior to the pyroelectric one under such conditions. This is an important result of Part II. Pyroelectric effect appears only when the temperature changes. At the constant temperature, no pyroelectric current is induced. However, photogalvanic current (charge generation) continues while the crystal is irradiated by light. It means, while the sample is irradiated, the surface charges are accumulated continuously. However, discharge of accumulated charges should be strictly controlled. This can open new applications of photogalvanic effect for crystal accelerator, X-ray generator, etc.

This program of research was financially supported by AOARD. We wish to acknowledge the kind support by Dr. Kumar Jata and Dr. Tammy Low, program managers of this proposed research. The author thanks Prof. J.K. Gimzewski and Dr. R.Wali of UCLA for fruitful discussions. He also thanks Drs. S.Takekawa and H.Hatano of NIMS for their cooperation.